



MR. KRISTOPHER JONATHAN WINIARSKI (Orcid ID : 0000-0002-2272-9770)

DR. WILLIAM PETERMAN (Orcid ID : 0000-0001-5229-9268)

Article type : Resource Article

Evaluation of ResistanceGA

Article type: Resource Article

Running title: Landscape resistance surface optimization

Evaluation of the R package ‘ResistanceGA’: A promising approach towards the accurate optimization of landscape resistance surfaces

Winiarski, K.J.^{1,2*}, Peterman, W.E.³, McGarigal, K.¹

1. Department of Environmental Conservation, University of Massachusetts, Amherst, Massachusetts, United States of America
2. Northeast Climate Adaptation Science Center, University of Massachusetts, Amherst, Massachusetts, United States of America
3. School of Environment and Natural Resources, Ohio State University, United States of America

*Corresponding author: withakri@gmail.com

This article has been accepted for publication and undergone full peer review but has not been through the copyediting, typesetting, pagination and proofreading process, which may lead to differences between this version and the Version of Record. Please cite this article as doi: [10.1111/1755-0998.13217](https://doi.org/10.1111/1755-0998.13217)

This article is protected by copyright. All rights reserved

Abstract

Understanding how landscape features affect gene flow has implications for numerous fields including molecular and evolutionary ecology. Despite this, modeling landscape resistance surfaces has remained a significant challenge. The R package ResistanceGA was developed to provide a framework for optimizing landscape resistance surfaces. In this study, we assessed ResistanceGA's ability to recover the true resistance surface under a variety of scenarios, including when the underlying surface: (i) had different levels of spatial autocorrelation and (ii) was transformed into a resistance surface using different functional transformations. These scenarios were evaluated with regard to varying sample size and varying levels of variance in the measure of genetic distance. We also assessed the ability of ResistanceGA to identify the true resistance surface among alternative correlated surfaces. In univariate simulations, correlation between the true and optimized resistance surfaces remained high with increased variance in genetic distance, but only when sample size was moderate to high (≥ 50). Model selection error was also driven by sample size with low type I error when simulations had moderate to high sample sizes, even with moderate to high variance in genetic distance and correlated alternative surfaces. ResistanceGA also performed well in multivariate simulations, but had more difficulty identifying the true data generating surfaces when genetic data was simulated using an agent-based approach (especially with individual based genetic data). Overall, our simulations highlight the ability of ResistanceGA to accurately optimize resistance surfaces but also underscore challenges in optimizing landscape resistance surfaces, especially with highly stochastic individual based data.

Key-words: CIRCUITSCAPE, gene flow, genetic algorithm, landscape genetics, resistance distance, ResistanceGA, resistance optimization.

Introduction

For a decade and a half, the field of landscape genetics has made important contributions to conservation biology, epidemiology and molecular and evolutionary ecology (Segelbacher et al.,

2010; Sork & Waits, 2010; Manel & Holderegger, 2013; Petren, 2013; Van Strien et al., 2014). The early success and rapid development of landscape genetics can be attributed to an active research community that has put a strong emphasis on identifying and addressing research needs and improving quantitative rigor (Balkenhol, Waits, & Dezzani, 2009; Epperson et al., 2010; Manel, Schwartz, Luikart, & Taberlet, 2003; Richardson, Brady, Wang, & Spear, 2016). However, the relative youth of the field has resulted in application of statistical methods and frameworks that have largely been borrowed from other disciplines (Dyer, 2015).

A primary focus of landscape genetics is to model landscape resistance surfaces that accurately represent the landscape characteristics acting as drivers or barriers to gene flow. Numerous simulation-based studies have been performed to address the many components of landscape resistance surface modeling such as spatial scale (Cushman & Landguth, 2010; Galpern, Manseau, & Wilson, 2012), contrast in landscape resistance (Cushman, Lewis, & Landguth, 2014; Shirk, Landguth, & Cushman, 2018), thematic resolution (Cushman & Landguth, 2010), landscape fragmentation (Cushman, Wasserman, Landguth, & Shirk, 2013), sampling regimes (Oyler-McCance et al., 2013), number of molecular markers and allelic richness (Landguth et al., 2012; Oyler-McCance et al., 2013), sample size (Landguth et al., 2012; Oyler-McCance et al., 2013), generational time (Landguth & Cushman, 2010a; Oyler-McCance et al., 2013a) and genetic non-equilibrium (Zeller et al., 2016; Shirk et al., 2018). Additionally, a multitude of analytical approaches to model landscape resistance have been proposed or developed (Cushman, McKelvey, Hayden, & Schwartz, 2006; Cushman et al., 2013; Franckowiak et al., 2017; Graves, Beier, & Royle, 2013; Gruber & Adamack, 2015; Peterman, 2018; Peterman et al., 2019; Row, Knick, Oyler-McCance, Lougheed, & Fedy, 2017; Shirk et al., 2018; Van Strien, Keller, & Holderegger, 2012; Zeller et al., 2016). Unfortunately, due to the nature of genetic and spatial data, many of these analytical approaches (e.g., derivatives of the Mantel test), when rigorously evaluated, have performed poorly (e.g., high type I error; Balkenhol et al., 2009; Legendre & Fortin, 2010; Graves et al., 2013; Manel & Holderegger, 2013; Cushman et al., 2013). These analytical issues have created a formidable challenge for modeling landscape resistance, and arguably has resulted in a bottleneck that has hindered continued advancement of the landscape genetics field (Richardson et al., 2016; Storfer, Murphy, Spear, Holderegger, & Waits, 2010).

In the field of landscape genetics, a true optimization of landscape resistance based on genetic distance data has eluded researchers since the origin of the discipline. Instead, researchers have had to resort to constrained grid search approaches (but see Wang, Savage, & Shaffer, 2009; Graves et al., 2013; Peterman, 2018), in which a limited parameter space is explored, resulting in a finite number of alternative models being assessed (Shirk, Wallin, Cushman, Rice, & Warheit, 2010). In contrast, ResistanceGA is an approach that provides true optimization of landscape resistance surfaces (Peterman, 2018). ResistanceGA is an R package that utilizes a genetic algorithm (R package GA; Scrucca, 2013) to optimize univariate continuous surfaces, categorical surfaces, or multivariate combinations (continuous and/or categorical) with pairwise genetic distance data. ResistanceGA's approach to optimization is unique as landscape resistance surfaces do not need to be defined a priori (Compton, McGarigal, Cushman, & Gamble, 2007) or pseudo-optimized (e.g., Shirk, Wallin, Cushman, Rice, & Warheit, 2010), as they are empirically optimized via the genetic algorithm. However, a rigorous examination of the algorithm's performance under widely varying but realistic scenarios had not been conducted until this study (a detailed description of the genetic algorithm is provided in the Materials and Methods).

Here, we simulated univariate and multivariate landscape resistance surfaces and evaluated ResistanceGA's ability to recover the true landscape resistance surface under a variety of scenarios, including: (i) the underlying surface having different levels of spatial autocorrelation and (ii) the underlying surface transformed into a landscape resistance surface using different functional transformations and evaluated these scenarios with varying sample size (i.e., number of sample point locations) and with multiple levels of variance in the measure of genetic distance between sample points. In addition, we evaluated model selection performance of ResistanceGA when alternative, often correlated, surfaces are present. These alternative surfaces were either spatially correlated environmental predictors, random surfaces uncorrelated with the true surface, or surfaces derived from both random and correlated surfaces. We also included the correct underlying surface measured at the wrong spatial scale as an alternative surface, as studies evaluating spatial surfaces at multiple spatial scales are becoming increasingly common (e.g., McGarigal, Wan, Zeller, Timm, & Cushman, 2016; Winiarski, Peterman, Whiteley, & McGarigal, 2019). Across all these scenarios, we evaluated

the ability of ResistanceGA to correctly identify the data generating resistance surface as well as the accuracy in optimizing a resistance surface.

Materials and Methods

To assess the performance of the R package ‘ResistanceGA’ we simulated landscape genetics data including i) univariate and multivariate landscape surfaces and resistance surfaces using a range of landscapes and resistance transformations and ii) variance added, population and individual genetic distance data using a range of sampling and biological parameters to assess the performance of the R package ‘ResistanceGA’, as outlined in Figure 1 and described below. The R code for simulating the landscape genetics data and the optimization of resistance surfaces to evaluate the performance of the R package ‘ResistanceGA’ for all simulations is provided online (<https://doi.org/10.6084/m9.figshare.12515584>).

Univariate Scenarios

For the univariate simulations, we evaluated 8 different landscape resistance surface scenarios representing unique combinations of spatial autocorrelation, functional transformations, and maximum landscape resistance values (Table 1). Thus, each scenario represented either a fine- or coarse-scaled fractal surface transformed into a unique landscape resistance surface based on the specified parameters of the resistance transformation. For each of these scenarios, we evaluated five different sample sizes (10, 25, 50, 75 and 90) and five different levels of variance ($SD = 0.001, 0.1, 0.25, 0.5$ and 1.25) in our surrogate measure of genetic distance, as described below. For each unique simulation, we conducted 50 iterations to reflect the stochastic processes involved in the generation of the fractal surfaces, distribution of sampling point locations, and our surrogate measure of genetic distance.

To evaluate model selection performance with the univariate simulations, we also developed and optimized alternative spatially correlated surfaces (5 levels) or smoothed surfaces (2 levels) to evaluate model selection performance in realistic cases where the spatial surfaces hypothesized to drive gene flow and genetic differentiation are often highly correlated (only for scenario #5; Table 1).

Multivariate Scenarios

For the multivariate simulations, we developed 4 different landscape resistance surface scenarios and conducted multivariate simulations in which the true landscape resistance surface was developed using two univariate surfaces. Multivariate simulation scenarios only differed in how the genetic distance data was simulated. Here, we evaluated simulations with genetic data simulated with two levels of variance in our surrogate measure of genetic distance ($SD = 0.5$ and 1.25) (75 sample points) and a population and individual agent-based simulation of genetic data (75 sample points for the population-based simulation and 200 sample points for the individual-based simulations). For each scenario, we conducted 50 iterations to reflect the stochastic processes involved in the generation of the fractal surfaces, distribution of sampling point locations, and the simulated genetic data.

To evaluate model selection performance with the multivariate simulations, we also developed and optimized three univariate (surface 1, surface 2, random surface) and four multivariate resistance surfaces (surface 1 + surface 2, surface 1 + random surface, surface 2 + random surface + surface 1 + surface 2 + random surface).

Simulating surfaces and transforming to a resistance surface

We simulated continuous spatially autocorrelated surfaces (hereafter referred to as fractal surfaces) using the R package ‘RandomFields’ (Schlather, M., Malinowski, A., Menck, P.J., Oesting, M., Strokorb, K., 2015). We created the fractal surfaces at two different extents (50^2 or 100^2 pixels; only 100^2 pixels with the univariate simulations) and two different levels of spatial autocorrelation (note: the univariate simulations results based on the performance metrics described below were similar between landscape extents; therefore, unless otherwise noted below we report only the results for the 50^2 pixel extent). Next, to create a true landscape resistance surface we transformed the original fractal surface(s) into a landscape resistance surface by specifying a functional transformation, shape and maximum resistance value using the `Resistance.tran` function in `ResistanceGA`.

For the univariate simulations, we had 8 different scenarios surfaces where we simulated a fine or coarse scale surface and then transformed that surface into a resistance surface using a functional transformation (Monomolecular or Inverse Ricker), shape (always equal to 3) and a maximum resistance value (50 or 200) (Table 1). For the multivariate simulations, we evaluated a single

combination of spatial autocorrelations, functional transformations, and maximum resistance values. Here, Surface 1 was parameterized as a fine-scale fractal surface (`RMexpscale` = 1) transformed using a Monomolecular transformation with a shape value of 3 and maximum resistance value of 100 and Surface 2 was parameterized as a coarse-scale fractal surface (`RMexpscale` = 25) transformed using an Inverse Ricker transformation with a shape value of 3 and a maximum resistance value of 100.

For scenario #5 of the univariate simulations, we also generated 5 correlated surfaces at varying levels of correlation (Pearson's r = 0.9, 0.7, 0.5, 0.3, and 0.1) to assess model selection performance using an analytical approach that retained the same pattern across the landscape and the original level of spatial autocorrelation. In addition, we also developed two additional surfaces by smoothing the original fractal surface with a Gaussian kernel at two different bandwidths (4 and 7 pixels) using the R package '`gridkernel`' (github.com/ethanplunkett).

To create a true multivariate landscape resistance surfaces for multivariate simulations we used `ResistanceGA`'s `Combine_Surfaces` function. Here, Surface 1 and Surface 2 were each transformed as described above for Scenario #5. The surfaces were then added together and then rescaled to create a single final landscape resistance surface with a minimum resistance value of 1 (Peterman, 2018). We also generated an additional random fractal surface which had an intermediate fractal scale (`RMexpscale` = 15) to include in the optimization and model selection analysis.

Sample points

For each univariate and multivariate simulation, sample points (10, 25, 50, 75 or 90 for the univariate simulations and 75 for the variance added and population-based multivariate simulations and 200 for the individual-based multivariate simulations) were probabilistically distributed across the true landscape resistance surface with the likelihood of sampling a pixel being inversely related to its landscape resistance value (Fig. 1). We excluded sample points from being placed on the edge of the surface (10 pixels for 50^2 pixel landscape and 20 pixels for the 100^2 pixel landscape) due avoid potential edge effects that can arise when calculating landscape resistance distances with `CIRCUITSCAPE` (Koen, Bowman, Sadowski, & Walpole, 2014; S1).

Pairwise genetic distances

- *Variance added genetic distance*

Variance added genetic distances (our surrogate of genetic distance) was developed by first measuring the resistance distance between all of the pairwise sample points on the true landscape resistance surface using CIRCUITSCAPE (McRae, Dickson, Keitt, & Shah, 2008) and then adding random normal noise. We evaluated five levels of variance in genetic distance for our univariate simulations ($SD = 0.001, 0.1, 0.25, 0.5$ and 1.25) and two with our multivariate simulations ($SD = 0.5$ and 1.25). This procedure allowed us to emulate varying strengths (from relatively weak to very strong) in the relationship between landscape resistance distances and genetic distance (Fig. 2; S1).

- *Agent-based genetic simulations*

Because our artificial genetic distance may not capture the stochastic properties of movement and gene flow processes between populations (e.g., genetic drift), we also derived genetic distance from a spatially explicit population and individual agent-based genetic simulation (note: only for our multivariate simulations). Agent-based population simulations were conducted with the R package PopGenReport (Adamack and Gruber, 2014) and agent-based individual based simulations were conducted with the CDPOP software (Landguth & Cushman, 2010b). For the population-based simulations we generated a landscape resistance surface and distributed 150 populations on the landscape as described above. Each population consisted of 30 individuals with an equal sex ratio. Females could produce 2 offspring at each time step. We tracked 30 microsatellite loci, each with 30 alleles and a mutation rate of 0.0005. We modeled a migration rate of 0.2. Individuals dispersing between populations could maximally disperse 12.5% of the maximum pairwise resistance distance between populations, and 25% of dispersing individuals could achieve this maximum dispersal distance. Simulations were run for 250 non-overlapping generations, after which we calculated chord distance between populations. Following simulations, 75 populations were randomly selected for analysis. These simulations generally created genetic data akin to our $SD = 1.25$ variance added metric (S2).

For the individual based simulations, we generated a landscape resistance surface and distributed 500 individuals with an equal sex ratio on the landscape as described above. Simulations were conducted

for 100 non-overlapping generations (Shirk et al., 2018) where we tracked 30 alleles at 30 microsatellite loci with a mutation rate of 0.0005 for each individual. All movement across the landscape followed an inverse square probability with the maximum movement distance being equal to the 2.5% quantile of all pairwise resistance distances across the landscape. Each female had a mean of 4 offspring, following a Poisson random process. Following simulations, we calculated Euclidean distance between individuals using 64 principle component axes (Shirk, Landguth, & Cushman, 2017), and then randomly selected 200 individuals for analysis.

Landscape resistance surface optimization

Optimization of the true landscape resistance surface and alternative landscape resistance surface(s) was performed using a genetic algorithm (R package GA; Scrucca, 2013) as implemented in the R package ResistanceGA (Peterman, 2018). Genetic algorithms are conceptually based on the theory of natural selection. As implemented in ResistanceGA, the algorithm uses unique combination of parameters (alleles) to transform a raster layer into a landscape resistance surface, which represents an "individual". Once a "population" of "individuals" is created, selection occurs whereby the landscape resistance surfaces that best explain pairwise genetic differentiation are retained and carried over to the next generation. In this way, the algorithm works iteratively towards identifying the best-fit landscape resistance surface(s) (i.e. the best-adapted). In our application, the optimization of a landscape resistance surface worked as follows:

- 1) The original fractal surface(s) was rescaled from 0 to 10.
- 2) A "population" of "individuals" was generated (equal to 15x the number of parameters to be optimized), in which each "individual" was assigned random values for the set of parameters needed to transform the rescaled fractal surface into a landscape resistance surface. The parameters included: (a) the functional transformation (Inverse-Reverse Monomolecular, Inverse-Reverse Ricker, Monomolecular, Reverse Monomolecular, Inverse Monomolecular, Inverse Ricker, and Distance), (b) the shape of the transformation (range = 0.5–14.5), and (c) the maximum resistance value of the transformation (range = 1– 2,500). For each "individual" or

unique set of parameter values, the fractal surfaces were transformed into a landscape resistance surface.

- 3) For each "individual" landscape resistance surface transformation, the pairwise resistance distance between sample point locations was calculated using CIRCUITSCAPE (McRae et al., 2008).
- 4) For each "individual", a linear mixed effects model with a maximum likelihood population effects parameterization (MLPE) was fit, in which our surrogate measure of genetic distance was treated as the response and the scaled and centered landscape resistance distance was treated as the predictor, and the identity of pairwise combinations of point locations was modeled as a random effect. The MLPE parameterization was used to account for the non-independence among the pairwise data (Clarke, Rothery, & Raybould, 2002) and has been shown to perform better than other regression-based approaches in this context (Shirk et al., 2018).
- 5) For each fitted model, Akaike information criterion adjusted for small sample size (AICc) was computed, with each model penalized by the overall complexity of the model and with sample size n equal to the number of sampled points (not the number of pairwise observations used in the MLPE model). Here, a single surface univariate model has a total of 4 parameters (intercept, transformation, shape and max value), and a multivariate two-surface model has a total of 7 parameters with any additional surface adding 3 more parameters (additional transformation, shape and max value).
- 6) For the "population" of fitted models, the top 5% of "individuals" (i.e., unique parameterizations) based on AICc were retained for the next "generation" to form the "reproducing population" and the remaining "individuals" were discarded.
- 7) For the selected "individuals", there was a probability of first a "mutation" (0.10) and then a "crossover" (0.85). Here, "mutation" involved the replacement of an "individual's" single parameter value with a random value, while "crossover" simulated breeding with another "individual" and the creation of a new "individual" by averaging parameter values of the two breeding "individuals".

- 8) Steps 2-7 were repeated until there was no improvement in AICc (default = 25 iterations without improvement; maximum number of iterations = 1,000).

Performance metrics

To evaluate ResistanceGA's performance in the univariate simulations, we computed several metrics. First, for each of the 50 iterations of the 200 unique simulations (8 different scenarios at 5 levels of sample size and 5 levels of variance in genetic distance), we computed Pearson's correlation (r) between the true and optimized landscape resistance surface and summarized the mean and standard error. Second, for scenario #5 and each of the 25 unique simulations (5 sample size levels and 5 levels of variance in genetic distance), we computed type I error rates, defined as the percentage of the 50 iterations in which the true data generating surface was not selected as the top surface when being evaluated against corresponding correlated or smoothed alternative surfaces, and the percentage of the 50 iterations in which each of the alternative surfaces was selected as the top surface. Third, for all of the 200 unique simulations (8 different scenarios at 5 levels of sample size and 5 levels of variance in genetic distance), we computed the percentage of the 50 iterations in which the correct functional transformation was selected by the optimization. Lastly, for those iterations in which the correct functional transformation was optimized, we also measured root mean square error (RMSE), bias and standard error (SE) of the optimized shape and maximum resistance parameters by scenario.

To evaluate ResistanceGA's performance in the multivariate simulations, we computed a similar set of metrics. First, for each of the 50 iterations of the two genetic variance added scenarios and the population and individual agent-based simulation, we computed Pearson's correlation (r) between the true and optimized landscape resistance surface and summarized the mean and standard deviation. Second, for each multivariate scenario, we computed the type I error rates, as defined above, and the percentage of the 50 iterations in which the true surfaces and each of the alternative surface(s) were selected as the best supported surface based on AICc model selection. Lastly, for each scenario, we also used a modified-bootstrap as an alternative and potentially more robust way to evaluate competing models (Peterman, 2018). Specifically, we used the Resist.boot function in ResistanceGA and defined a subsample of 75% of the pairwise response and landscape resistance distance data from the optimized multi-surface model (without replacement) and ran 1,000 bootstrap

iterations in which the function refit the MLPE model for randomly selected pairwise observations. For each of the 50 iterations for each multivariate scenario, the Resist.boot function calculated the percentage of the 1,000 bootstrap iterations in which each model was selected as the top model as well as the average AICc weight across bootstrap iterations. Results were summarized across the 50 iterations.

Results

Correlation between true and optimized landscape resistance surfaces

For the univariate simulations, patterns in the correlations between the true and optimized landscape resistance surfaces were generally consistent across all of the landscape resistance surface scenarios (S3) and spatial extents (S4) that we evaluated. Correlations were relatively high (>0.8) across all levels of variance in genetic distance when the sample size was ≥ 50 (Fig. 3). If the sample size was ≤ 25 , the correlation between surfaces depended strongly on the level of variance in genetic distance. Although the pattern of variation across sample size and level of variance was similar between the fine-scale fractal surfaces (landscape resistance surface scenarios 1-4; Table 1) and coarse-scale fractal surfaces (landscape resistance surface scenarios 5-8; Table 1), the correlations were consistently higher with the coarse-scale surfaces (S3). Similarly, the correlations were consistently higher with the Monomolecular versus the Inverse Ricker transformations (S3). The maximum resistance value (50 vs. 200) used to develop the true landscape resistance surface appeared to have no overall effects on correlation between the true and optimized landscape resistance surfaces (S3).

For the multivariate simulations, correlations were generally high (range of 0.73 to 0.93) between the true and optimized landscape resistance surfaces at all levels of variance in genetic distance and with the population and individual agent-based simulations of genetic data (Table 2), but recall that all of these simulations were run with a relatively large sample size (75 sample locations variance added/population-based genetic simulations or 200 individual-based genetic simulations).

Model selection error

In univariate analyses, type 1 error rates were relatively low (<25%) and AICc model weights for the true landscape resistance surface were correspondingly high (>0.75) across levels of variance in genetic distance when the sample size was ≥ 50 , except at the highest level of variance ($SD = 1.25$; Figs. 5–6). Conversely, when sample size was ≤ 25 , type I error rates were consistently relatively high (>25%) (Fig. 5) and AICc model weights for the true landscape resistance surface varied substantially (as low as 0.15) across levels variance in genetic distance (Fig. 6). However, when the top model was not the true landscape resistance surface (i.e., type I error), the top model was usually one of the landscape resistance surfaces highly correlated ($r \geq 0.7$) with the true landscape resistance surface or the moderately smoothed version of the true landscape resistance surface. This pattern was consistent except at the highest levels of variance in genetic distance when the sample size was small (Fig. 7).

For the multivariate simulations using our surrogate measure of genetic distance and population genetic simulations, type I error rates were 20–30% across the scenarios assessed and were reduced by 6–14% when using the modified-bootstrap to conduct model selection (Table 2; Fig. 8). Thus, when using bootstrap model selection, the true multivariate landscape resistance surface was selected as the top model > 75 percent of the time. For the individual agent-based genetic simulations, type I error rates significantly increased (78% type I error) and did not decrease when using the modified-bootstrap to conduct model selection (Table 2; Fig. 8). Notably, surface 2 alone was often selected as the top model in the individual agent-based analyses (>50% of iterations) (Fig. 8). Model weights were relatively high in the low genetic variance scenario ($SD = 0.5$) and decreased with the high genetic variance scenario ($SD=1.25$) and the population and individual-based genetic simulation scenarios (Table 2). In the individual-based genetic simulation scenario AICc weights were only ~0.24 for the true multi surface model, but this is due to surface 2 so frequently being identified as the better supported surface (Table 2). To further diagnose the discrepancy between individual and population agent-based simulations, we plotted the correlation between genetic distance and true resistance distance with the correlation between the true and optimized resistance distance measures (Fig. 4). All population simulations resulted in genetic distance data that was highly correlated (> 0.7) with the true distance. In contrast, the correlation in individual simulations was generally 0.5–0.7. It also appears that correct model selection is in part affected by the optimization achieving a correlation

>0.75 between the true and optimized resistance distances. In the noisier and more stochastic individual simulations, this was often not the case.

Optimization of functional transformation and shape and maximum resistance parameters

For the univariate simulations, patterns in the percentage of the iterations in which the correct functional transformation was selected by the optimization across sample sizes and levels of variance in genetic distance were generally consistent across all of the landscape resistance surface scenarios that we evaluated (S5). Simulations with moderate to high sample sizes (≥ 50) had a high percentage (>75%) of iterations optimized using the true transformation at all levels of variance in genetic distance when the correct transformation was the Inverse Ricker, and at all but the highest levels of variance when the correct transformation was the Monomolecular (e.g., Fig. 9). Generally, sensitivity to sample size and level of variance in genetic distance was greater for Monomolecular versus Inverse Ricker transformations (e.g., Fig. 9). In particular, when the strength of the relationship between landscape resistance distance and genetic distance was very strong (i.e., low variance in genetic distance) and the functional relationship was Monomolecular, the correct transformation was almost always selected by the optimization; however, when the strength of the relationship between landscape resistance distance and genetic distance was very weak (i.e., high variance in genetic distance), an incorrect transformation was more often selected. More specifically, when the true transformation was Monomolecular, and it was not selected by the optimization, the selection usually favored the Inverse Ricker or Inverse-Reverse Monomolecular (S6). Similarly, when the true transformation was Inverse Ricker and it was not selected by the optimization, the selection usually favored the Inverse-Reverse Monomolecular (S7).

The accuracy and precision of the optimized shape and maximum resistance parameters, as reflected by the RMSE, bias and SE of the estimates, decreased rapidly as sample size decreased and level of variance in genetic distance increased across all scenarios (Table 3; S8-S13). However, the magnitude and rate of deterioration in these two measures varied considerably among scenarios, and much more so than with the correlation and type I error. In particular, the accuracy and precision of the shape parameter was considerably greater for the scenarios based on the Inverse Ricker transformation than those based on the Monomolecular transformation (S8, S10, S12). This pattern

was true for the maximum resistance parameter as well, but the differences between transformations were much less dramatic (S9, S11, S13). In addition, bias in the estimate of maximum resistance decreased markedly as the true maximum resistance value increased; indeed, bias was negligible across all scenarios when the true maximum resistance was 200 (S11).

Discussion

Across the broad range of simulations evaluated, we confirmed the ability of ResistanceGA to effectively optimize landscape resistance surfaces, so long as the sample size is relatively large (generally ≥ 50). With our univariate scenarios, the performance in most metrics deteriorated rapidly for sample sizes ≤ 25 , and the deterioration was especially evident when the strength in the relationship between landscape resistance distance and genetic distance was relatively weak (e.g., $SD \geq 0.5$ in our surrogate measure of genetic distance; Fig. 2). ResistanceGA performed well at sample sizes ≤ 25 only when landscape resistance was a strongly correlated with genetic distance (e.g., $SD \leq 0.25$ in our surrogate measure of genetic distance; Fig. 2). The performance of ResistanceGA also appears to be quite robust to changes in the input surface characteristics, at least in terms of degree of spatial autocorrelation and spatial extent. The functional relationship between the original continuous surface and the landscape resistance surface is expressed through the parameterization of the selected transformation function, and we found that there was a tradeoff between selecting the correct transformation function and the accuracy and precision of the corresponding parameter estimates. Lastly, our use of ResistanceGA's modified-bootstrap model selection procedure to evaluate alternative models with our multivariate simulations substantially reduced type I error (6–14%) in all multivariate scenarios, except in the individual-based genetic simulations where type I error remained the same. Hence, this modified-bootstrap approach shows promise for model selection with spatially correlated alternative landscape resistance surfaces and suggests that applying a more “traditional” model selection approach based simply off AICc and model weights should be used with caution.

We found our simulation results to be both consistent and inconsistent with previous landscape resistance surface modeling simulation studies.

- Spatial extent and grain size

In contrast to our simulation findings, where we find little effect of the spatial extent of the simulated resistance surface, Cushman & Landguth (2010) found that both grain (pixel size) and spatial extent had small but statistically significant effects on estimates of inferred gene flow. Galpern et al. (2012) also found that spatial grain affected the results, with evidence of the landscape driving gene flow only when spatial layers were evaluated at spatial grains coarser than the original 200m grain size. These findings warrant additional simulations to evaluate the effect of spatial grain on the performance of ResistanceGA.

- Sample size

Our findings generally agree with previous simulation studies that found that sample size has a strong influence on type I error and correlation between the “true” and selected landscape resistance surface (Landguth et al., 2012; Oyler-McCance et al., 2013; Row et al., 2017; Shirk et al., 2018). It is worth noting that the sample sizes needed to accurately select the true landscape resistance surface was much less in our study using ResistanceGA (Fig. 3) than reported in these previous simulation studies (>200 in Landguth et al., 2012; Oyler-McCance, Fedy, & Landguth, 2013), although differences in simulation approaches (e.g., sampling schemes) between studies make it difficult to make direct comparisons. Nevertheless, it is encouraging that ResistanceGA’s optimization may perform well with fewer observations than previously used analytical approaches (Shirk et al., 2018). The relatively poor performance of landscape resistance surfaces optimized with low sample sizes in our study and these others is somewhat sobering given the plethora of landscape genetics studies using relatively low sample sizes.

- Identifying the correct functional transformation

ResistanceGA was more successful in identifying the Inverse Ricker function as the correct transformation compared to the Monomolecular when the sample size was small and the relationship between landscape resistance distance and genetic distance was weak, but the accuracy and precision of the shape and maximum landscape resistance distance parameters was lower. In addition, ResistanceGA estimated the maximum resistance of the landscape resistance surface with much less bias when the true landscape resistance surface had a higher maximum resistance value (S11),

suggesting that the algorithm performs better when there is greater contrast in the landscape resistance surface.

Overall, it appears that the only way to ensure that the optimized transformation is an accurate and precise translation of the input layer is with a large sample size, and this becomes increasingly true as the strength of the relationship between landscape resistance distance and genetic distance weakens.

Future work

With flexible optimization comes the potential to overfit. Genetic data is inherently noisy with a large amount off variation in pairwise genetic distance across geographic or resistance distances. There is potential for the flexible transformations and multisurface optimization ability of ResistanceGA to overfit to this noise. There currently are no great strategies or safeguards against overfitting. The modified bootstrap procedure used in our multivariate model selection are an effort to minimize this, with some success in population-based simulations. Model ranking using AIC or AICc is largely unexplored. Currently, AICc of MLPE models fit with ResistanceGA is calculated based off the number of spatial locations sampled (not the number of pairwise comparisons in the data) and penalized by the number of parameters being estimated. Calculation of AICc for these optimized surfaces could potentially be improved upon. An ideal solution to prevent overfitting would be to conduct a true bootstrap analysis or a leave-one-out cross validation where models are repeatedly optimized with subsets of the data. However, such an approach is computationally not feasible with ResistanceGA.

One potential caveat of our study, and conclusions drawn about ResistanceGA's abilities, is our use of a synthetic genetic distance measure. By adding different levels of random noise to the true resistance relationship, we were able to more precisely control variation in our simulations to better understand the effects of sample size and surface correlation when optimizing landscape resistance surfaces. We note, however, that random noise likely does not capture the pairwise patterns that emerge in real population genetic data sets. This was evident in our multivariate scenarios where we also simulated population and individual agent-based genetic data. The stochastic nature of individuals moving between populations, as well as isolation and drift, resulted in data that exhibited

a greater amount of heteroscedasticity (S2). The population and individual agent-based genetic data proved more difficult to correctly optimize than our surrogate measure of genetic distance and ultimately resulted in lower overall correlation with the true resistance surface and higher type I error rates. Nonetheless, correlations with the true resistance surface were still relatively high (~0.74). Type I error rates were relatively low for the population-based simulation, but were very high in our individual-based genetic simulations where one of the two true surfaces was most often selected in isolation. Our general conclusion from the equivalent comparison between our surrogate genetic distance measure and the population and individual agent-based genetic measure is that our use of a variance-added genetic measure throughout the study likely resulted in somewhat inflated accuracy measures, and that our highest variance measure ($SD = 1.25$) is most comparable to empirical genetic data sets.

Conclusions

Our simulation study provides evidence that ResistanceGA is able to effectively optimize landscape resistance surfaces under a wide range of realistic landscape genetics scenarios, making it a valuable and powerful tool for future landscape genetic analyses. Nonetheless, there are limitations, and our study serves as a reminder that advances in analytical methods are not a panacea for making inference from challenging data sets (e.g., small sample sizes, high variance in genetic data). The highest level of variance assessed in our simulation was intended to represent a challenging scenario (i.e. a weak relationship between landscape resistance distance and genetic distance) and, as expected, type I error rates were quite high (25 to 90 % depending on sample size) under these conditions with our univariate simulations. However, even under these worst-case scenarios the correlation between the optimized landscape resistance surface and the true landscape resistance surface remained quite high (> 0.80) so long as the sample size was ≥ 50 . This suggests that secondary analyses requiring a parameterized landscape resistance surface (e.g., corridor mapping or reserve design) may not be too adversely affected by type I error if the sample size is relatively large. However, we found that caution is needed when interpreting the drivers of landscape resistance especially with individual-based genetic data.

Our study has shed light on how sample size, degree of spatial autocorrelation and model selection approaches with spatially correlated alternative surfaces affects ResistanceGA's performance when optimizing landscape resistance surfaces. There are numerous other aspects of population genetics and landscape features that can affect landscape genetics inferences, such as landscape composition, number of genetic markers, and sampling design that still need to be investigated through simulations with ResistanceGA. There are also unknowns regarding parameterization of the genetic algorithm used in ResistanceGA and whether changes in default parameters could potentially improve inference or decrease computational time (e.g., What is the best mutation rate, crossover rate and number of "individuals" in a population? How much of an improvement in model fit is justifiable for producing another generation?). The performance of ResistanceGA in relation to these and other features is unknown but is an area of relevant future research that will require a more direct simulation of genetic processes to assess. In addition, multivariate simulations should be expanded to more than two layers to be more realistic.

Acknowledgements

Ethan Plunkett provided an approach and helped develop R code to simulate spatially correlated continuous surfaces. Brad Compton and Ethan Plunkett aided with running simulations on the University of Massachusetts Landscape Ecology Lab computer cluster. Simulations were also completed using the Ohio State University's Supercomputer Center (1987). Support for WEP was provided by the USDA National Institute of Food and Agriculture, Hatch project 1020979.

Authors' Contributions

KW, KM and WP designed the simulation. KW and WP conducted simulations and analyses. KW and KM led the writing with contributions from WP.

References

- Balkenhol, N., Waits, L. P., & Dezzani, R. J. (2009). Statistical approaches in landscape genetics: an evaluation of methods for linking landscape and genetic data. *Ecography*, 32(5), 818–830. doi: 10.1111/j.1600-0587.2009.05807.x
- Clarke, R. T., Rothery, P., & Raybould, A. F. (2002). Confidence limits for regression relationships between distance matrices: Estimating gene flow with distance. *Journal of Agricultural, Biological, and Environmental Statistics*, 7(3), 361–372. doi: 10.1198/108571102320
- Compton, B. W., McGarigal, K., Cushman, S. A., & Gamble, L. R. (2007). A Resistant-Kernel Model of Connectivity for Amphibians that Breed in Vernal Pools. *Conservation Biology*, 21(3), 788–799. doi: 10.1111/j.1523-1739.2007.00674.x
- Cushman, S. A., & Landguth, E. L. (2010a). Scale dependent inference in landscape genetics. *Landscape Ecology*, 25(6), 967–979. doi: 10.1007/s10980-010-9467-0
- Cushman, S. A., & Landguth, E. L. (2010b). Spurious correlations and inference in landscape genetics. *Molecular Ecology*, 19(17), 3592–3602. doi: 10.1111/j.1365-294X.2010.04656.x
- Cushman, S. A., McKelvey, K. S., Hayden, J., & Schwartz, M. K. (2006). Gene Flow in Complex Landscapes: Testing Multiple Hypotheses with Causal Modeling. *The American Naturalist*, 168(4), 486–499. doi: 10.1086/506976
- Cushman, S., Lewis, J., & Landguth, E. (2014). Why Did the Bear Cross the Road? Comparing the Performance of Multiple Resistance Surfaces and Connectivity Modeling Methods. *Diversity*, 6(4), 844–854. doi: 10.3390/d6040844
- Cushman, S., Wasserman, T., Landguth, E., & Shirk, A. (2013). Re-Evaluating Causal Modeling with Mantel Tests in Landscape Genetics. *Diversity*, 5(1), 51–72. doi: 10.3390/d5010051
- Dyer, R. J. (2015). Is there such a thing as landscape genetics? *Molecular Ecology*, 24(14), 3518–3528. doi: 10.1111/mec.13249
- Epperson, B. K., Mcrae, B. H., Scribner, K., Cushman, S. A., Rosenberg, M. S., Fortin, M.-J., ... Dale, M. R. T. (2010). Utility of computer simulations in landscape genetics. *Molecular Ecology*, 19(17), 3549–3564. doi: 10.1111/j.1365-294X.2010.04678.x

- Franckowiak, R. P., Panasci, M., Jarvis, K. J., Acuña-Rodriguez, I. S., Landguth, E. L., Fortin, M.J., & Wagner, H. H. (2017). Model selection with multiple regression on distance matrices leads to incorrect inferences. *PLOS ONE*, 12(4), e0175194. doi: 10.1371/journal.pone.0175194
- Galpern, P., Manseau, M., & Wilson, P. (2012). Grains of connectivity: analysis at multiple spatial scales in landscape genetics. *Molecular Ecology*, 21(16), 3996–4009. doi: 10.1111/j.1365-294X.2012.05677.x
- Graves, T. A., Beier, P., & Royle, J. A. (2013). Current approaches using genetic distances produce poor estimates of landscape resistance to interindividual dispersal. *Molecular Ecology*, 22(15), 3888–3903. doi: 10.1111/mec.12348
- Gruber, B., & Adamack, A. T. (2015). landgenreport: a new r function to simplify landscape genetic analysis using resistance surface layers. *Molecular Ecology Resources*, 15(5), 1172–1178. doi: 10.1111/1755-0998.12381
- Koen, E. L., Bowman, J., Sadowski, C., & Walpole, A. A. (2014). Landscape connectivity for wildlife: development and validation of multispecies linkage maps. *Methods in Ecology and Evolution*, 5(7), 626–633. doi: 10.1111/2041-210X.12197
- Landguth, E. L., & Cushman, S. A. (2010a). cdpop: A spatially explicit cost distance population genetics program. *Molecular Ecology Resources*, 10(1), 156–161. doi: 10.1111/j.1755-0998.2009.02719.x
- Landguth, E. L., & Cushman, S. A. (2010b). cdpop: A spatially explicit cost distance population genetics program. *Molecular Ecology Resources*, 10(1), 156–161. doi: 10.1111/j.1755-0998.2009.02719.x
- Landguth, E. L., Fedy, B. C., Oyler-McCance, S. J., Garey, A. L., Emel, S. L., Mumma, M., ... Cushman, S. A. (2012). Effects of sample size, number of markers, and allelic richness on the detection of spatial genetic pattern. *Molecular Ecology Resources*, 12(2), 276–284. doi: 10.1111/j.1755-0998.2011.03077.x
- Legendre, P., & Fortin, M.-J. (2010). Comparison of the Mantel test and alternative approaches for detecting complex multivariate relationships in the spatial analysis of genetic data. *Molecular Ecology Resources*, 10(5), 831–844. doi: 10.1111/j.1755-0998.2010.02866.x

- Manel, S., & Holderegger, R. (2013). Ten years of landscape genetics. *Trends in Ecology & Evolution*, 28(10), 614–621. doi: 10.1016/j.tree.2013.05.012
- Manel, S., Schwartz, M. K., Luikart, G., & Taberlet, P. (2003). Landscape genetics: combining landscape ecology and population genetics. *Trends in Ecology & Evolution*, 18(4), 189–197. doi: 10.1016/S0169-5347(03)00008-9
- McGarigal, K., Wan, H. Y., Zeller, K. A., Timm, B. C., & Cushman, S. A. (2016). Multi-scale habitat selection modeling: a review and outlook. *Landscape Ecology*, 31(6), 1161–1175. doi: 10.1007/s10980-016-0374-x
- McRae, B. H., Dickson, B. G., Keitt, T. H., & Shah, V. B. (2008). Using Circuit Theory to Model Connectivity in Ecology, Evolution, and Conservation. *Ecology*, 89(10), 2712–2724. doi: 10.1890/07-1861.1
- Oyler-McCance, S. J., Fedy, B. C., & Landguth, E. L. (2013a). Sample design effects in landscape genetics. *Conservation Genetics*, 14(2), 275–285. doi: 10.1007/s10592-012-0415-1
- Oyler-McCance, S. J., Fedy, B. C., & Landguth, E. L. (2013b). Sample design effects in landscape genetics. *Conservation Genetics*, 14(2), 275–285. doi: 10.1007/s10592-012-0415-1
- Peterman, W. E. (2018). ResistanceGA: An R package for the optimization of resistance surfaces using genetic algorithms. *Methods in Ecology and Evolution*, 9(6), 1638–1647. doi: 10.1111/2041-210X.12984
- Peterman, W. E., Winiarski, K. J., Moore, C. E., Carvalho, C., S., Gilbert, A. L., & Spear, S. F. (2019). A comparison of popular approaches to optimize landscape resistance surfaces. *Landscape Ecology*, 34(9), 2197–2208. doi: 10.1007/s10980-019-00870-3
- Petren, K. (2013). The Evolution of Landscape Genetics. *Evolution*, 67(12), 3383–3385. doi: 10.1111/evo.12278
- Richardson, J. L., Brady, S. P., Wang, I. J., & Spear, S. F. (2016). Navigating the pitfalls and promise of landscape genetics. *Molecular Ecology*, 25(4), 849–863. doi: 10.1111/mec.13527
- Row, J. R., Knick, S. T., Oyler-McCance, S. J., Lougheed, S. C., & Fedy, B. C. (2017). Developing approaches for linear mixed modeling in landscape genetics through landscape-directed dispersal simulations. *Ecology and Evolution*, 7(11), 3751–3761. doi: 10.1002/ece3.2825

Schlather, M., Malinowski, A., Menck, P.J., Oesting, M., Strokorb, K. (2015). Analysis, Simulation and Prediction of Multivariate Fields with Package RandomFields. *Journal of Statistical Software*, 63(8).

Scrucca, L. (2013). **GA** : A Package for Genetic Algorithms in R. *Journal of Statistical Software*, 53(4). doi: 10.18637/jss.v053.i04

Segelbacher, G., Cushman, S. A., Epperson, B. K., Fortin, M.J., Francois, O., Hardy, O. J., ... Manel, S. (2010). Applications of landscape genetics in conservation biology: concepts and challenges. *Conservation Genetics*, 11(2), 375–385. doi: 10.1007/s10592-009-0044-5

Shirk, A. J., Landguth, E. L., & Cushman, S. A. (2017). A comparison of individual-based genetic distance metrics for landscape genetics. *Molecular Ecology Resources*, 17(6), 1308–1317. doi: 10.1111/1755-0998.12684

Shirk, A. J., Wallin, D. O., Cushman, S. A., Rice, C. G., & Warheit, K. I. (2010a). Inferring landscape effects on gene flow: a new model selection framework. *Molecular Ecology*, 19(17), 3603–3619. doi: 10.1111/j.1365-294X.2010.04745.x

Shirk, A. J., Wallin, D. O., Cushman, S. A., Rice, C. G., & Warheit, K. I. (2010b). Inferring landscape effects on gene flow: a new model selection framework. *Molecular Ecology*, 19(17), 3603–3619. doi: 10.1111/j.1365-294X.2010.04745.x

Shirk, Andrew J., Landguth, E. L., & Cushman, S. A. (2018). A comparison of regression methods for model selection in individual-based landscape genetic analysis. *Molecular Ecology Resources*, 18(1), 55–67. doi: 10.1111/1755-0998.12709

Sork, V. L., & Waits, L. (2010). Contributions of landscape genetics – approaches, insights, and future potential. *Molecular Ecology*, 19(17), 3489–3495. doi: 10.1111/j.1365-294X.2010.04786.x

Storfer, A., Murphy, M. A., Spear, S. F., Holderegger, R., & Waits, L. P. (2010). Landscape genetics: where are we now? *Molecular Ecology*, 19(17), 3496–3514. doi: 10.1111/j.1365-294X.2010.04691.x

van Strien, M. J., Keller, D., & Holderegger, R. (2012). A new analytical approach to landscape genetic modelling: least-cost transect analysis and linear mixed models. *Molecular Ecology*, 21(16), 4010–4023. doi: 10.1111/j.1365-294X.2012.05687.x

- Accepted Article
- van Strien, M. J., Keller, D., Holderegger, R., Ghazoul, J., Kienast, F., & Bolliger, J. (2014). Landscape genetics as a tool for conservation planning: predicting the effects of landscape change on gene flow. *Ecological Applications*, 24(2), 327–339. doi: 10.1890/13-0442.1
- Wang, I. J., Savage, W. K., & Shaffer, H. B. (2009). Landscape genetics and least-cost path analysis reveal unexpected dispersal routes in the California tiger salamander (*Ambystoma californiense*). *Molecular Ecology*, 18(7), 1365–1374. doi: 10.1111/j.1365-294X.2009.04122.x
- Winiarski, K. J., Peterman, W. E., Whiteley, A. R., & McGarigal, K. (n.d.). Multiscale resistant kernel surfaces derived from inferred gene flow: An application with vernal pool breeding salamanders. *Molecular Ecology Resources*, 0(0). doi: 10.1111/1755-0998.13089
- Zeller, K. A., Creech, T. G., Millette, K. L., Crowhurst, R. S., Long, R. A., Wagner, H. H., ... Landguth, E. L. (2016). Using simulations to evaluate Mantel-based methods for assessing landscape resistance to gene flow. *Ecology and Evolution*, 6(12), 4115–4128. doi: 10.1002/ece3.2154

Tables

Table 1. Univariate scenarios for simulating the true landscape resistance surface. Scenarios represent unique combinations of: i) RMexpscale, which controls the level of spatial autocorrelation in the simulated continuous fractal surface, ii) transformation for converting input surface values to landscape resistance values, iii) shape and iv) maximum resistance parameters associated with the functional transformation. All scenarios were modeled at 5 different sample sizes and 5 different variance levels.

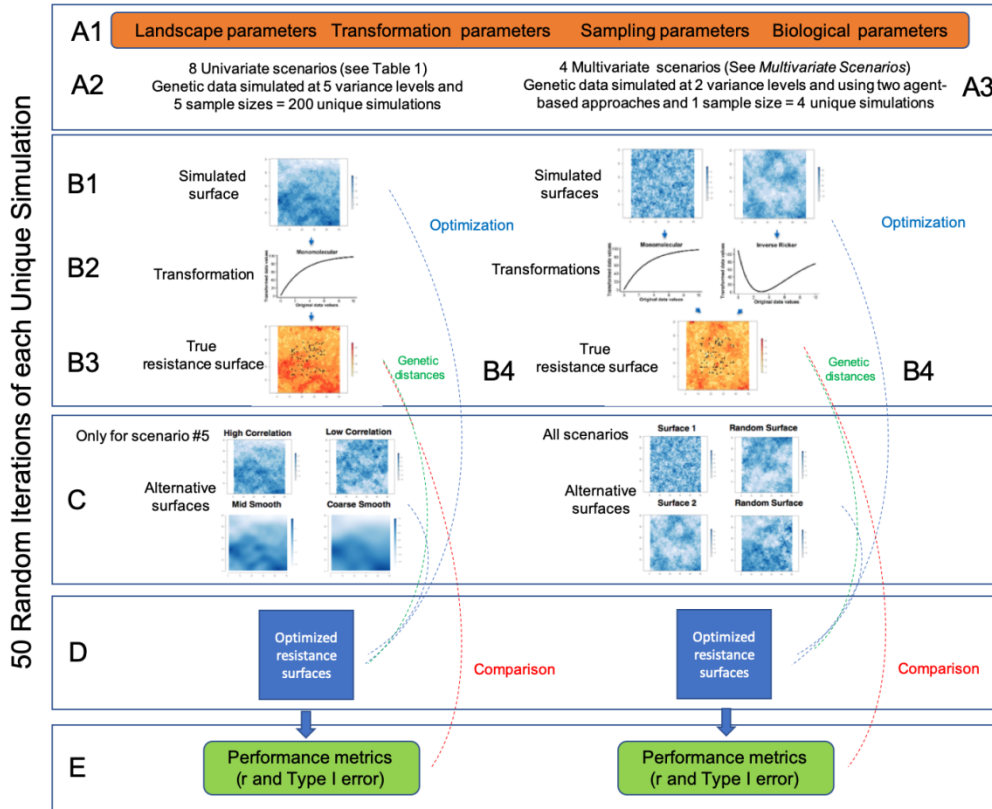
Scenario	RMexpscale	Transformation	Shape	Max Resistance	Sample Size	Variance Added Level
1	1	Monomolecular	3	50	10 / 25 / 50 / 75 / 90	0.001 / 0.1 / 0.25 / 0.5 / 1.25
2	1	Inverse Ricker	3	50	10 / 25 / 50 / 75 / 90	0.001 / 0.1 / 0.25 / 0.5 / 1.25
3	1	Monomolecular	3	200	10 / 25 / 50 / 75 / 90	0.001 / 0.1 / 0.25 / 0.5 / 1.25
4	1	Inverse Ricker	3	200	10 / 25 / 50 / 75 / 90	0.001 / 0.1 / 0.25 / 0.5 / 1.25
5	25	Monomolecular	3	50	10 / 25 / 50 / 75 / 90	0.001 / 0.1 / 0.25 / 0.5 / 1.25
6	25	Inverse Ricker	3	50	10 / 25 / 50 / 75 / 90	0.001 / 0.1 / 0.25 / 0.5 / 1.25
7	25	Monomolecular	3	200	10 / 25 / 50 / 75 / 90	0.001 / 0.1 / 0.25 / 0.5 / 1.25
8	25	Inverse Ricker	3	200	10 / 25 / 50 / 75 / 90	0.001 / 0.1 / 0.25 / 0.5 / 1.25

Table 2. Performance metrics for the multivariate simulations by either level of variance (standard deviation or genetic simulation) in genetic distance or population and individual agent-based genetic simulations including: i) Pearson's correlation (r) between the true and optimized resistance surfaces, ii) type I error rate (%), defined as the percentage of 50 iterations in which the true surface was not selected as the top model, and iii) Model weight and standard deviation of the true optimized surface. Means and standard deviations were derived from the 50 random iterations.

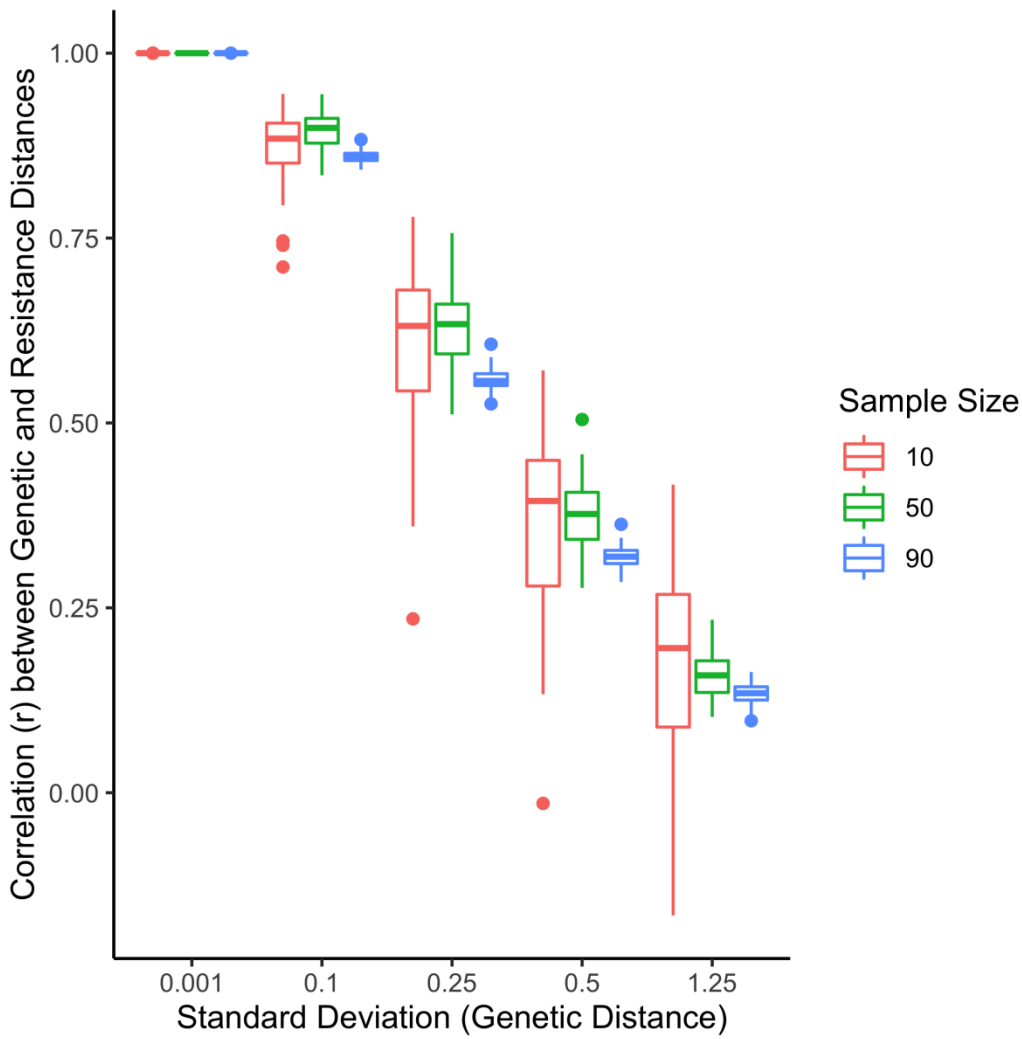
Performance Metric	0.5	1.25	Population	Individual
Correlation (Mean/SD)	0.93 (0.05)	0.86 (0.11)	0.73 (0.24)	0.75 (0.10)
Percent type I error rate (no bootstrap / bootstrap)	20% / 6%	20% / 14%	30% / 24%	78% / 78%
Mean true model AICc weight (SD)	0.71 (0.14)	0.41 (0.13)	0.58 (0.28)	0.24 (0.37)

Table 3. Root mean square error, bias and standard error (SE) for the optimized shape and maximum resistance parameters for the univariate scenarios by level of variance (standard deviation) in genetic distance for the univariate scenarios #S1-S4 (Table 1; scenarios simulating a fine fractal surface) with a sample size of 50.

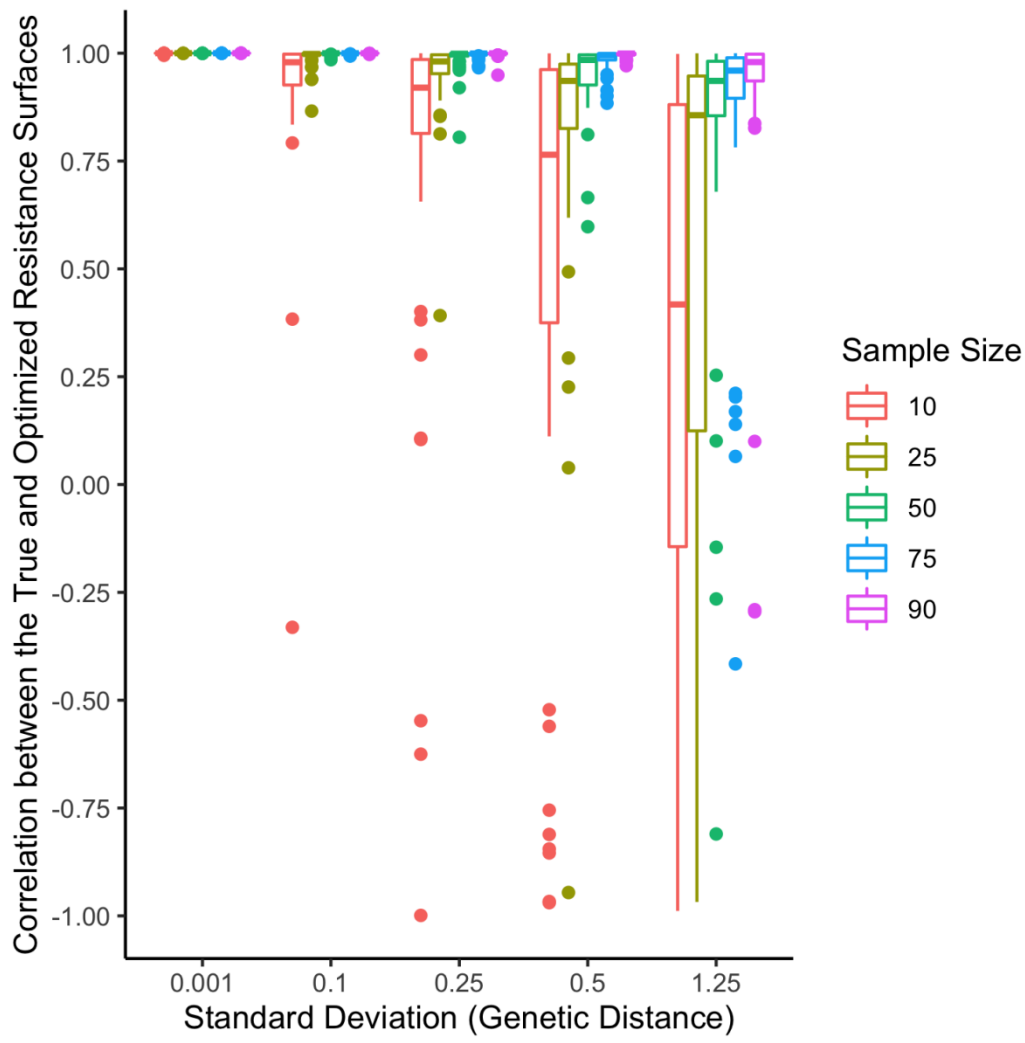
		Variance Level in Genetic Distance (Standard Deviation)									
		Shape					Max Resistance				
Scenario		0.001	0.1	0.25	0.5	1.25	0.001	0.1	0.25	0.5	1.25
RMSE	S1	0.01	0.1	0.32	0.55	1.02	14.5	35.9	43.07	43.8	80.74
	S2	0.02	0.02	0.02	0.03	0.07	7.64	16.49	17.22	18.76	32.07
	S3	0	0.12	0.35	0.8	1.12	15.43	23.23	25.94	39.61	53.66
	S4	0.01	0.01	0.01	0.02	0.05	5.76	14.06	16.98	21.7	32.22
	S1	0.01	0.04	0.22	0.36	0.4	1.22	3.79	4.04	3.56	5.26
	S2	0.02	0.02	0.02	0.01	0.02	0.4	1.31	1.22	1.23	2.08
	S3	0	0.07	0.29	0.68	0.42	0.32	0.14	0.11	0.4	0.58
	S4	0	0	0	0	0.01	0.04	0.14	0.21	0.17	0.39
	S1	0.01	0.1	0.3	0.52	0.97	11.55	23.27	29.32	30.42	43.95
	S2	0.02	0.02	0.02	0.03	0.07	7.03	13.44	14.73	16.05	26.32
	S3	0	0.11	0.32	0.7	1.07	12.43	22.86	25.7	36.63	44.42

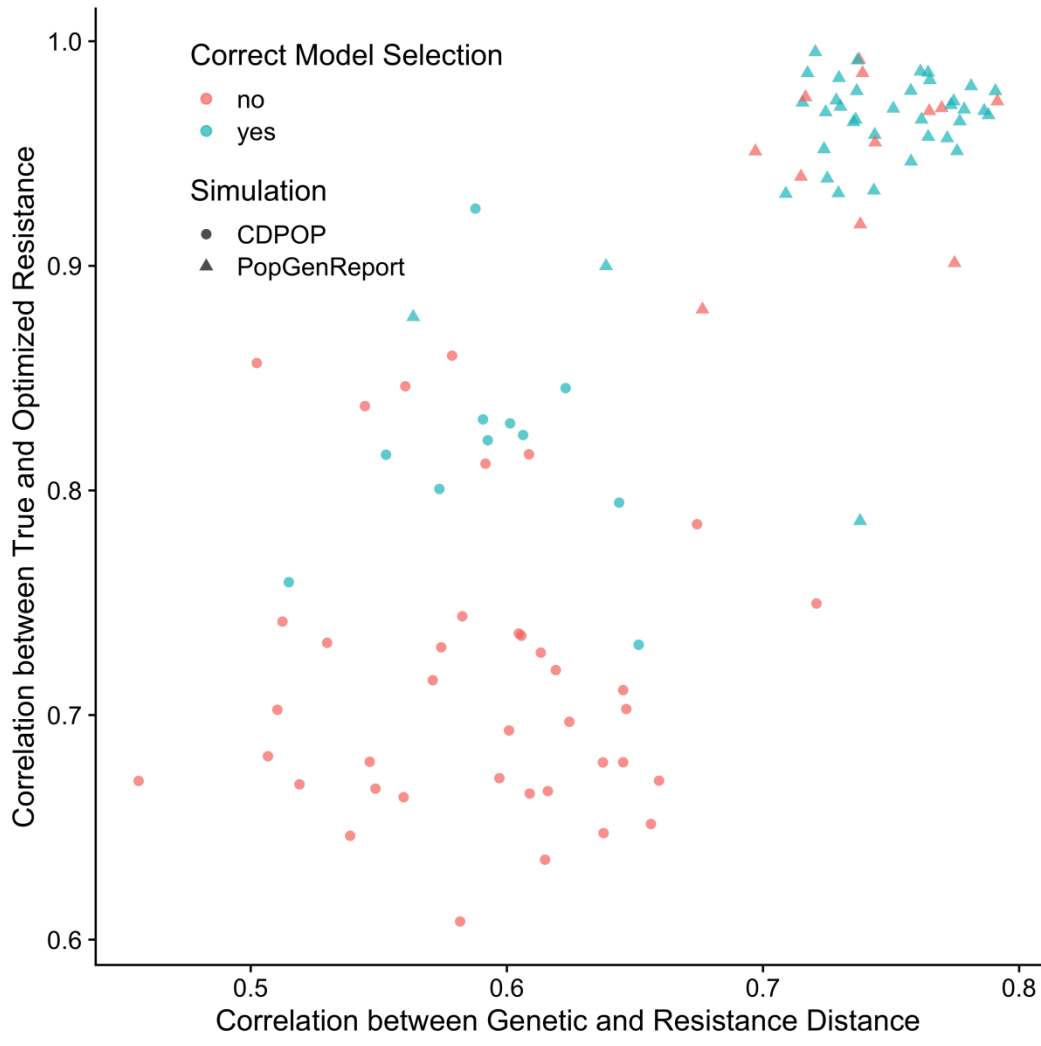


men_13217_f1.png

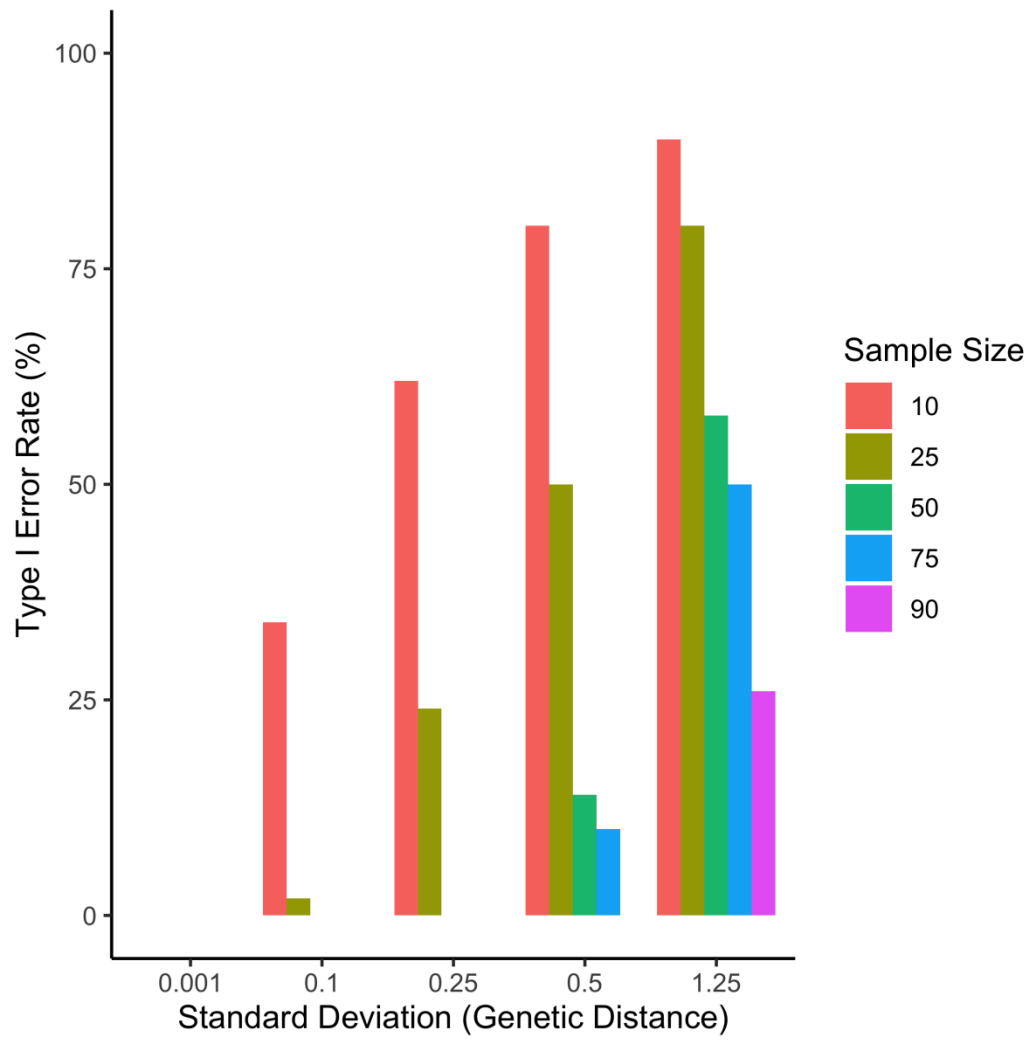


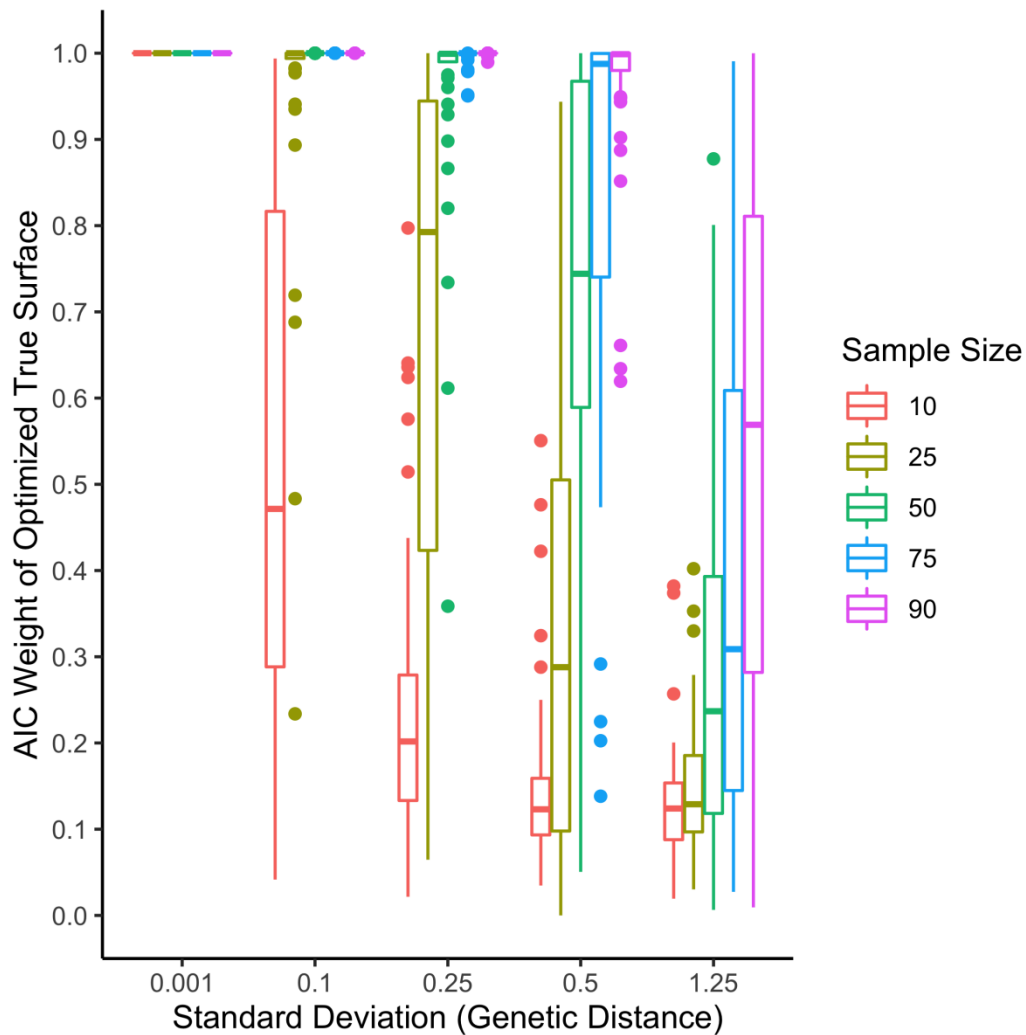
men_13217_f2.png

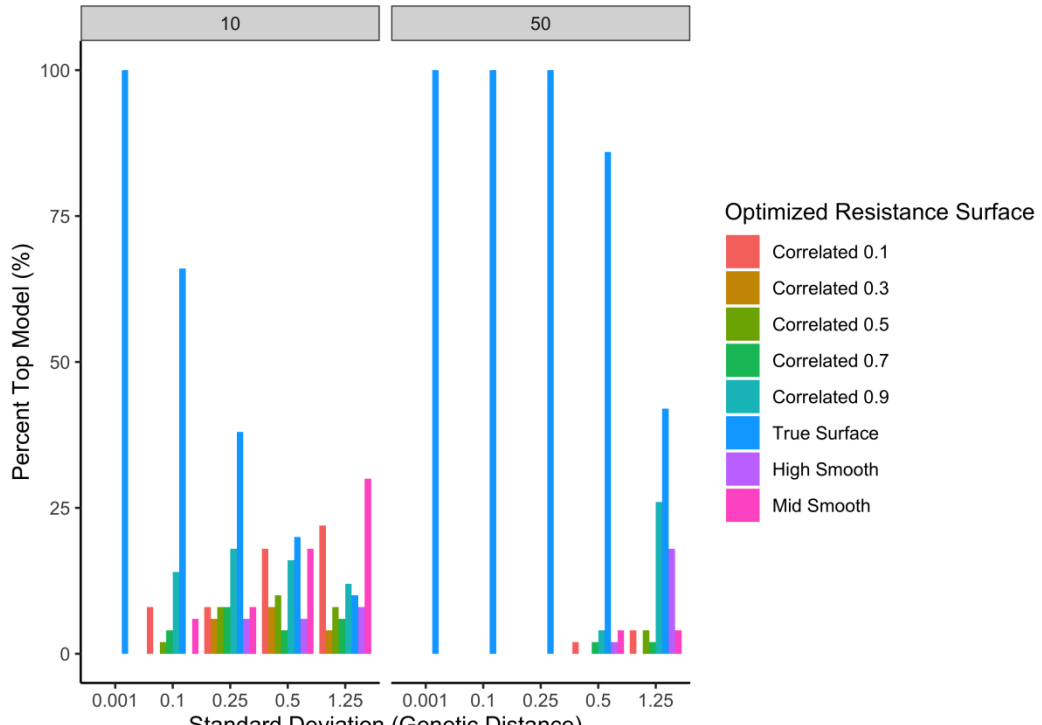




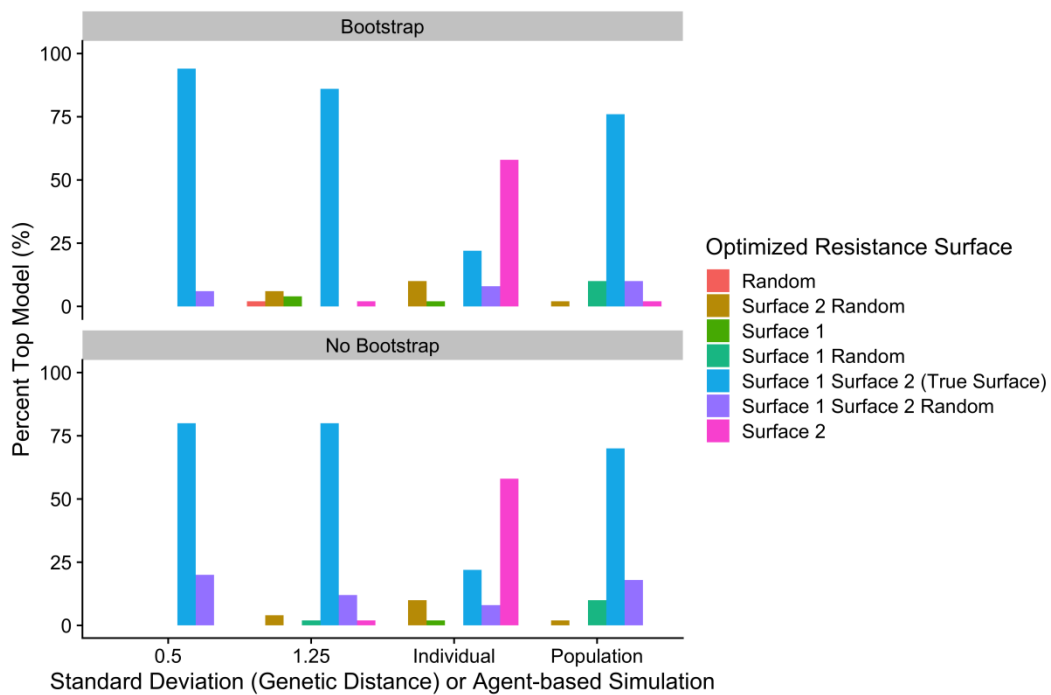
men_13217_f4.png



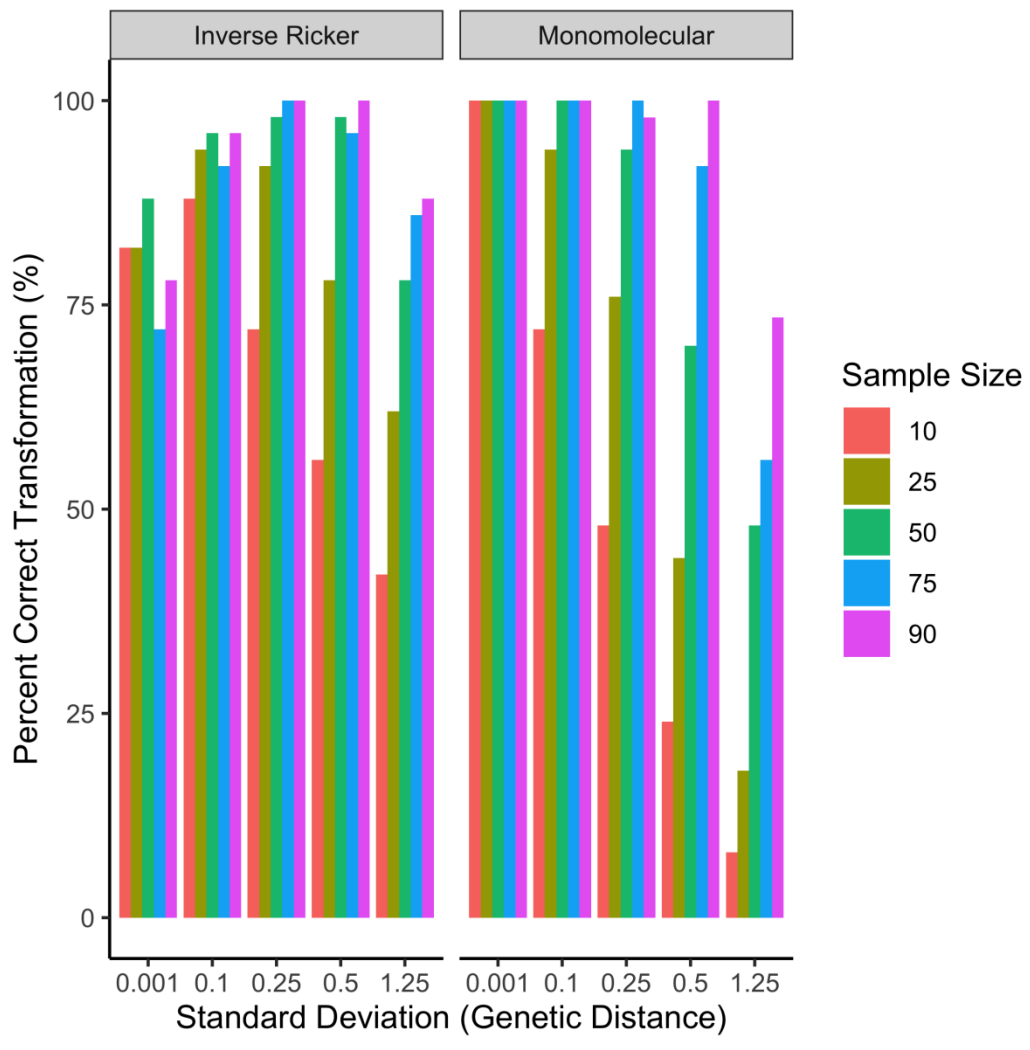




men_13217_f7.png



men_13217_f8.png



men_13217_f9.png